SCIENTIFIC REPORTS

OPEN

SUBJECT AREAS:
ATTOSECOND SCIENCE
NONLINEAR OPTICS
APPLIED PHYSICS
X-RAYS

Received
12 February 2013

Accepted
13 February 2013

Published
11 March 2013

Correspondence and requests for materials should be addressed to A.L. (anne.lhuillier@fysik.lth.se)

Efficient high-order harmonic generation boosted by below-threshold harmonics

F. Brizuela[1], C. M. Heyl[1], P. Rudawski[1], D. Kroon[1], L. Rading[1], J. M. Dahlström[2], J. Mauritsson[1], P. Johnsson[1], C. L. Arnold[1] & A. L'Huillier[1]

[1]Department of Physics, Lund University, P. O. Box 118, SE-22100 Lund, Sweden, [2]Atomic Physics, Fysikum, Stockholm University, AlbaNova University Center, SE-10691 Stockholm, Sweden.

High-order harmonic generation (HHG) in gases has been established as an important technique for the generation of coherent extreme ultraviolet (XUV) pulses at ultrashort time scales. Its main drawback, however, is the low conversion efficiency, setting limits for many applications, such as ultrafast coherent imaging, nonlinear processes in the XUV range, or seeded free electron lasers. Here we introduce a novel scheme based on using below-threshold harmonics, generated in a "seeding cell", to boost the HHG process in a "generation cell", placed further downstream in the focused laser beam. By modifying the fundamental driving field, these low-order harmonics alter the ionization step of the nonlinear HHG process. Our dual-cell scheme enhances the conversion efficiency of HHG, opening the path for the realization of robust intense attosecond XUV sources.

The interaction of intense laser pulses with atomic or molecular gas media leads to the generation of harmonics of the laser light, up to very high orders[1]. These harmonics are locked in phase, giving rise to attosecond bursts of XUV light. The simplicity of the experimental technique, together with the progress in ultrafast laser technology, has promoted HHG sources as essential tools in many laboratories; opening, in particular, the field of attosecond science[2]. However, HHG suffers from low conversion efficiency, owing partly to phase mismatches in the nonlinear medium that prevent efficient build up of the macroscopic field[3–6], but mostly to the weak response of the individual atoms to the field.

The atomic response to an external driving field can be described by a three-step model [Fig. 1(a)]: First, a bound electron tunnel-ionizes into the continuum; second, it is accelerated by the laser field; and finally, it recombines with the parent ion upon field reversal, emitting an XUV photon[7,8]. The electron trajectories can be grouped in two families, named the long and the short, depending on the excursion time of the electron and generated in intervals II and III of Fig. 1(a), respectively. The most interesting from a practical point-of-view are the short trajectories, which lead to collimated and spectrally narrow emission. Unfortunately, these trajectories start at times close to the zero-crossings of the driving electric field, suffering from very low quantum-tunneling probability.

Altering the driving electric field at the subcycle level[9] provides a way of modifying the single atom response. This has been investigated mainly by adding the second harmonic field[10–13], thus breaking the symmetry between consecutive half cycles. In contrast, odd-order harmonics modify the HHG process while maintaining the half-cycle symmetry. In a pioneering work, Watanabe and coworkers[14] investigated the influence of the third harmonic (TH) on single ionization and HHG in Ar, obtaining an enhancement of up to a factor of ten for the 27–31 harmonics. Also, a few theoretical works discuss the influence of the TH on the enhancement of the yield[15,16] and/or the extension of the cutoff energy[17–19]. Another approach to enhance the signal by modify the single atom response is to control the time of ionization by using attosecond pulse trains to initialize the three-step process via single photon absorption[20–23].

In this letter, we demonstrate a simple and robust, yet powerful enhancement scheme based on a dual gas-cell setup [Fig. 1(b)]. We study HHG in neon using a high-energy (~20 mJ), near-infrared fundamental field, loosely focused in a long gas cell, resulting in high-order harmonics in the 40–100 eV range, with a typical energy of 10 nJ per harmonic order. The addition of a high-pressure Ar gas cell before the generation cell produces a large enhancement in the Ne signal, as seen in Fig. 1(c). We experimentally and theoretically show that the observed enhancement is due to below-threshold, low-order harmonics which modify the fundamental field in such a way that the contribution of the short trajectories is increased.

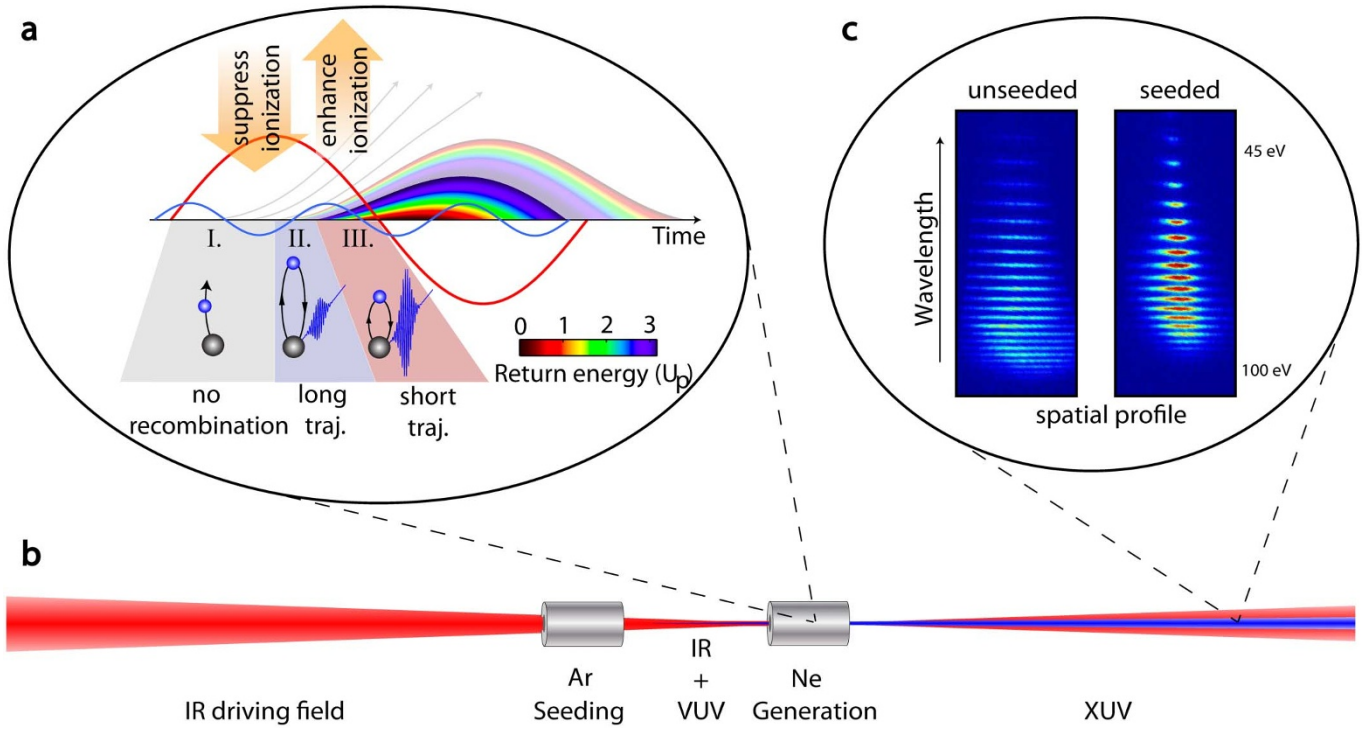

Figure 1 | HHG in a dual gas-cell. (a) Schematic classical trajectories for a sinusoidal driving field (red line). The colors indicate the return energy of the electrons in units of the ponderomotive energy U_p. Modifying the driving field by adding an odd harmonic field (blue line) can lead to an enhanced ionization probability for short trajectories (interval III) while suppressing the ionization of non-contributing electrons (intervals I and II), as indicated by the arrows. (b) Schematic experimental setup. Low-order harmonics generated in the seeding cell co-propagate with the fundamental into the generation cell and modify the HHG process. (c) Comparison of a typical HHG spectrum from a neon-filled generation cell obtained using only the fundamental field; and a spectrum obtained combining the fundamental field with low-order harmonics generated in the argon-filled seeding cell. In the latter case, the harmonic yield for the plateau harmonics is enhanced while the cutoff energy and the divergence are reduced.

Results

In our experiment, the generation cell is placed approximately at the laser focus while the seeding cell is located a few centimeters before (see Methods). The gas pressures in the cells can be independently adjusted and are typically a few mbar in the generation cell (Ne) and up to tens of mbar in the seeding cell (Ar). In Fig. 2(a–c), HHG spectra from neon are plotted as a function of the seeding pressure for three different driving intensities. When no gas is present in the seeding cell, standard Ne spectra are obtained. As the seeding pressure increases, the signal from the neon cell decreases until it is almost completely suppressed. At higher pressures, the neon spectra reappear and are significantly enhanced in the 50 – 80 eV region while the maximum photon energy slightly shifts to lower harmonic orders.

Figure 2(d) shows harmonics generated in the seeding cell. Harmonics with energies above the ionization threshold are not present at pressures where the enhancement in the generation cell occurs, and therefore are not responsible for the signal boost through single-photon ionization[20–23]. At these pressures, only low-order harmonics are efficiently generated in the seeding cell, indicating that they are responsible for the seeding process.

In order to validate our interpretation, we performed numerical simulations for both cells. In the generation cell, we simulated the seeded HHG process using the strong-field approximation

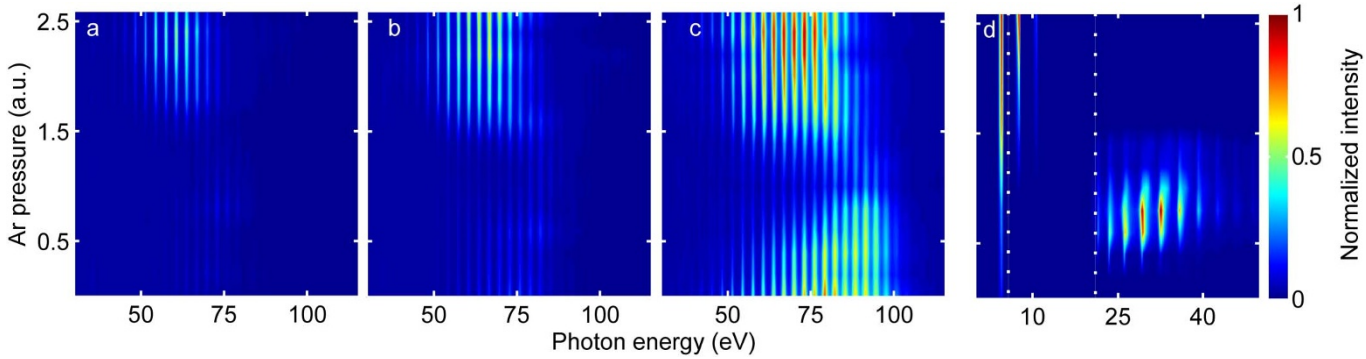

Figure 2 | Experimental HHG spectra. (a-c) Spectra from the generation cell as a function of the pressure in the seeding cell at three driving intensities 2.7, 3.5, and 4.4 × 10^{14} W/cm^2, respectively. The spectra were obtained using argon in the seeding cell and neon, at a fixed pressure, in the generation cell. The data were normalized to the most intense enhanced neon spectrum. (d) Low- (3–7) and high-order harmonics from the seeding cell as a function of Ar pressure. The dotted lines indicate regions measured independently with different detectors. Each region was normalized to the highest intensity in the corresponding spectral range.

(SFA)[15,16,24,25] (see Methods). The total field can be written as

$$E(t) = E_0 \left[\sin(\omega t) + \sum_{q\omega < I_p} r_q \sin\left(q\omega t + \Delta\varphi_q\right) \right], \qquad (1)$$

where E_0 is the amplitude of the fundamental field, ω its frequency, I_p the ionization energy, r_q the ratio between the fundamental and qth harmonic field, and $\Delta\varphi_q$ their relative phase. Although all harmonics below the ionization threshold of Ar may influence the enhancement phenomenon, we considered only the TH, which is the most intense one (we omit the subscript 3 below). A simulated HHG spectrum in neon with $|r|^2 = 0.01$, is shown in Fig. 3(a) as a function of $\Delta\varphi$. A relative phase of ~1 rad leads to an enhanced ionization probability, since the electrical field is increased at the time where the short electron trajectories are born [interval III in Fig. 1(a)]. Furthermore, the electric field amplitude is reduced around the peak of the fundamental field leading to suppressed probability for non-contributing trajectories (intervals I, II) and to an improved macroscopic situation since plasma dispersion and depletion effects are minimized[4,5]. When $\Delta\varphi \approx 1 \pm \pi$, the situation is reversed and HHG is suppressed compared to the unseeded case.

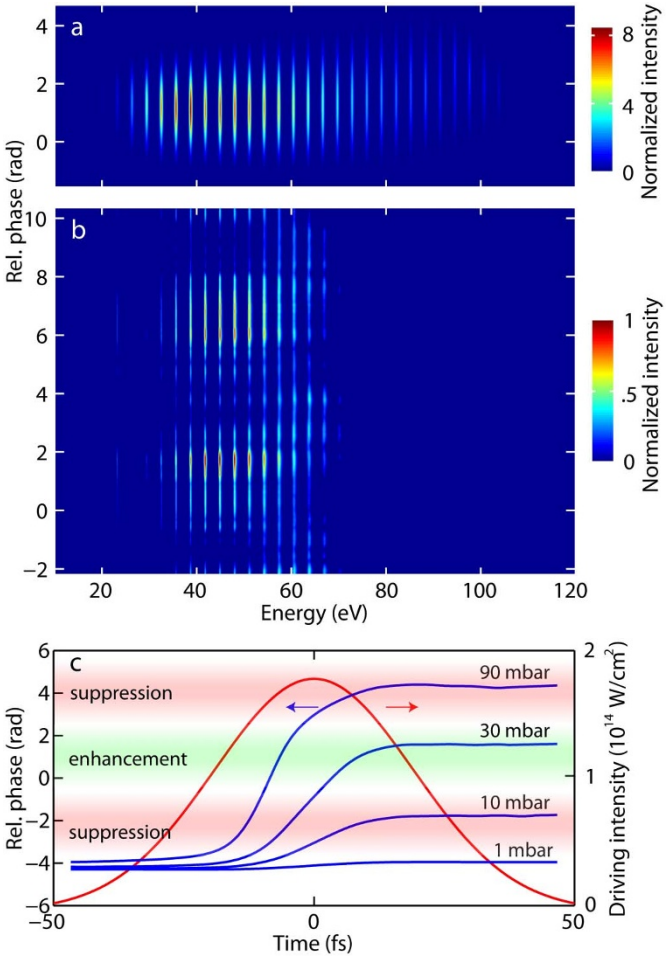

Figure 3 | Influence of the relative (ω, 3ω) phase in HHG. (a) SFA spectra as a function of $\Delta\varphi$ in the generation cell, normalized to the unseeded spectrum. Only the contribution of the short trajectory is considered. An effective grating response is included to mimic the experimental conditions. (b) Experimental results with the TH generated in a crystal, normalized to the highest signal. (c) Propagation simulations in the seeding cell: $\Delta\varphi$ at the exit of the cell as a function of time for different pressures.

We experimentally confirmed the dependence of the HHG signal on $\Delta\varphi$ by studying HHG using a combination of the fundamental and the TH generated in a crystal[14]. To control the delay between the two fields, we used a Michelson interferometer with the TH produced in one arm. Our results, plotted in Fig. 3(b), show a strong delay dependence of the harmonic yield. However, we could not increase the overall HHG efficiency compared to the dual-cell scheme, since a large fraction of the fundamental field was needed for the TH generation and consequently lost for HHG.

In the seeding cell, we examined the pressure dependence of both low-order and high-order harmonic generation. Our calculations[26] confirm the experimental observation that HHG in Ar peaks at a certain pressure (~10 mbar) which corresponds to optimized phase matching[27], while below-threshold harmonics continue to increase up to pressures as high as 100 mbar. We also investigated the propagation of the fundamental and TH fields in a high pressure cell[28] (see Methods). This allowed us to examine their phase relation after the seeding cell and to eliminate the relatively weak reshaping of the fundamental field in our experimental conditions as possible cause for the enhancement. As Fig. 3(c) shows, for high enough seeding pressures, $\Delta\varphi$ will be between 0 and 2 radians during part of the laser pulse, leading to a gated enhancement mechanism.

Discussion

As in any enhancement scheme, a key question is whether our method is advantageous over "usual" HHG optimization, which can be achieved for example by using looser focusing, optimizing the position of the focus in the cell, or adjusting the pressure in the gas cell[4,29,30]. Ideally, one would like to compare optimized HHG and optimized seeded HHG for a given fundamental pulse energy. This is not easy to realize experimentally, so we choose to benchmark seeded HHG against optimized unseeded HHG, with ~10 nJ at 63 eV (41st harmonic).

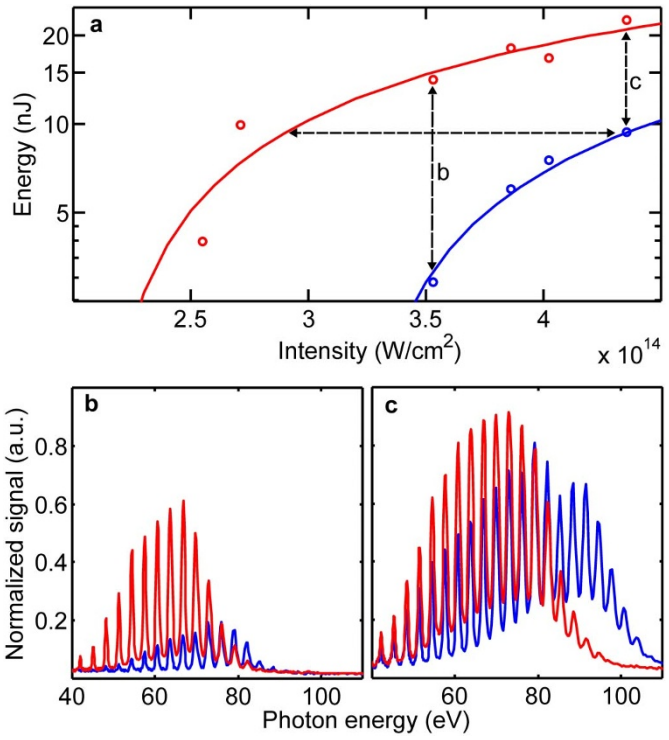

Figure 4 | Optimization of HHG. (a) 41st harmonic energy as a function of the driving intensity for seeded (red) and unseeded (blue) HHG. Unseeded HHG is optimized at the maximum intensity. (b, c) Corresponding experimental spectra at 3.5 and 4.4 × 10^{14} W/cm^2, respectively.

Figure 4(a) compares the 41st harmonic signal in the seeded and unseeded cases as a function of the driving intensity. The intensity required for saturating seeded HHG is only half that needed for unseeded HHG. This explains the reduction of the cutoff energy and the lower divergence for the harmonics. The enhancement factor depends on the driving intensity [Fig. 4(b,c)]. For the 41st harmonic, it varies from five at 3.5×10^{14} W/cm^2 (and even higher at lower intensity) to two at 4.4×10^{14} W/cm^2. By further optimizing seeded HHG (e.g. by changing the focusing conditions) one should be able to obtain an even larger increase compared to unseeded HHG. The higher efficiency together with the lower divergence leads to a brighter source of XUV light.

In summary, we have studied the effect of seeding HHG using harmonics generated in a separate gas cell and showed that low-order harmonics are responsible for the resulting enhancement. The combined electric field preferentially enhances the short trajectories while suppressing depletion and plasma dispersion effects. The required phase difference between the fundamental and the low-order harmonics is obtained by adjusting the pressure in the seeding cell, thus modifying the free-electron dispersion. Our method is not limited to the gas combination presented here. Experimentally we have observed an increased harmonic yield for a variety of gas combinations, and even when the same gas is used in both cells. Our simulations show that the enhancement can be scaled far above one order of magnitude by increasing the low-order harmonic intensity, for example by using longer cells, higher pressures or gases with higher nonlinearities. This also leads to a shorter temporal gate, of interest for single attosecond pulse generation.

Methods

Experimental setup. The harmonics were generated using 45 fs pulses, centered at 800 nm. The gas cells used in this setup were 1 cm long with a diameter of 1 mm. The injection of gas into the cell was synchronized with the laser repetition rate (10 Hz) and the delay between the gas injection and the laser pulse was optimized for each cell. In the experiments, seeding cell pressure and pulse energy were the parameters investigated. The generation cell pressure was set for the best phase-matching conditions for Ne at the highest laser intensity intensity (4.4×10^{14} W/cm^2), corresponding to less than 10 mbar. The focus position was adjusted in order to optimize HHG in the generation cell. The cell separation was 15 mm with the generation-cell located at focus (f = 4 m). Nevertheless, larger separations, up to 50 mm yielded similar results. The cells were mounted on motor-controlled XYZ stages with motorized XY tilt capabilities. The cells could be removed completely from the IR field. A CCD camera was used to align each cell to the laser and observation of the spectra at the best phase-matching conditions were used to evaluate the tilt of each cell. The same Ne spectra from the generation cell could be obtained though the evacuated seeding cell or with the seeding cell removed from the beam path. The same was true for the seeding cell where Ar spectra could be obtained under both conditions. The pressure and intensity controls were automated to scan the region of interest. At each experimental condition 10 single-shot spectra were measured and averaged. The harmonic orders were calibrated using the absorption edge of an Al-foil filter. The fundamental intensity was estimated from the cutoff of the unseeded Ne spectra.

Numerical simulations. *Generation cell.* The influence of a weak third harmonic field on the HHG process was simulated by solving the time dependent Schrödinger Equation within the strong field approximation. The quasi-classical action for the electron motion in the continuum

$$S(\vec{p},t,t_0) = \int_{t_0}^{t} dt' \left(\frac{\left[\vec{p} - e\vec{A}(t')\right]^2}{2m} + I_p \right) \tag{2}$$

is calculated for a combined vector potential of the fundamental field and a weak parallel auxiliary field consistent with the field definition in Eq. (1). t_0 and t correspond to the tunneling and recombination times for an electron with canonical momentum $\vec{p}$, I_p is the ionization potential, and $\vec{A}$ the vector potential of the field. We approximate the HHG dipole as[24]

$$\begin{aligned} x(t) = i \int_0^\infty d\tau \left(\frac{\pi}{\epsilon + i\tau/2} \right)^{3/2} & d_x^*(p_{st}(t,\tau) - A_x(t)) \\ & \times d_x(p_{st}(t,\tau) - A_x(t-\tau)) E(t-\tau) \\ & \times \exp[-iS_{st}(t,\tau)] F(\tau) + c.c., \end{aligned} \tag{3}$$

where a stationary phase approximation is performed over momentum, with $p_{st}(t,\tau) = [E(t) - E(t-\tau)]/\tau$, where $\tau = t - t_0$ is the excursion time in the continuum. We also insert a filter function $F(\tau)$ to select the short trajectory: $F(\tau) \approx 1$ for $\tau < 0.65T$ and $F(\tau) \approx 0$ for $\tau > 0.65T$, where $0.65T$ corresponds to the position of the cutoff. The integral in Eq. (3) is then evaluated numerically on a finite grid followed by a numerical Fourier transform for the dipole emission.

Seeding cell. We performed calculations which combine the solution of the time-dependent Schrödinger equation in a single-active electron approximation and propagation in a partially ionized medium[26,5] using a slowly-varying envelope approximation. Our main goal was to examine the influence of the pressure both for low-order and high-order harmonic generation in conditions mimicking the experiment. We found a maximum for HHG at around 10 mbar, while below-threshold, low-order harmonics which are not reabsorbed in the medium continue to increase up to very high pressures (100 mbar).

The generation of the third harmonic in the seeding cell was simulated using a (3 + 1)-dimensional, unidirectional, nonlinear envelope equation[28]. The complete frequency dependent dispersion relation is considered, enabling to propagate the fundamental and the third harmonic simultaneously. It is numerically integrated using a split-step technique, where the linear contributions, such as dispersion and diffraction are treated in k-transverse frequency space, while the nonlinear part, taking into account the Kerr effect, third-harmonic generation as well as plasma dispersion and plasma defocusing is treated in normal space. The method is described in detail in[28]. The calculated phase variation is mainly due to plasma dispersion effects. There are also small contributions from the geometrical phase acquired along the seeding cell as well pressure-dependent third harmonic phase matching.

1. Popmintchev, T. *et al.* Bright Coherent Ultrahigh Harmonics in the keV X-ray Regime from Mid-Infrared Femtosecond Lasers. *Science* **336**, 1287–1291 (2012).
2. Krausz, F. & Ivanov, M. Attosecond Physics. *Rev. Mod. Phys.* **81**, 163 (2009).
3. Constant, E. *et al.* Optimizing High Harmonic Generation in Absorbing Gases: Model and Experiment. *Phys. Rev. Lett.* **82**, 1668 (1999).
4. Kazamias, S. *et al.* Global Optimization of High Harmonic Generation. *Phys. Rev. Lett.* **90**, 193901 (2003).
5. Gaarde, M. B., Tate, J. L. & Schafer, K. J. Macroscopic aspects of attosecond pulse generation. *J. Phys. B* **41**, 132001 (2008).
6. Willner, A. *et al.* Efficient control of quantum paths via dual-gas high harmonic generation. *New J. Phys.* **13**, 113001 (2011).
7. Corkum, P. B. Plasma perspective on strong field multiphoton ionization. *Phys. Rev. Lett.* **71**, 1994–1997 (1993).
8. Schafer, K. J., Yang, B., DiMauro, L. F. & Kulander, K. C. Above threshold ionization beyond the high harmonic cutoff. *Phys. Rev. Lett.* **70**, 1599 (1993).
9. Wirth, A. *et al.* Synthesized Light Transients. *Science* **334**, 195–200 (2011).
10. Eichmann, H. *et al.* Polarization-dependent high-order two-color mixing. *Phys. Rev. A* **51**, R3414 (1995).
11. Mauritsson, J. *et al.* Attosecond Pulse Trains Generated Using Two Color Laser Fields. *Phys. Rev. Lett.* **97**, 013001 (2006).
12. Kim, I. J. *et al.* Highly Efficient High-Harmonic Generation in an Orthogonally Polarized Two-Color Laser Field. *Phys. Rev. Lett.* **94**, 243901 (2005).
13. Raz, O., Pedatzur, O., Bruner, B. D. & Dudovich, N. Spectral caustics in attosecond science. *Nat. Phot.* **6**, 170 (2012).
14. Watanabe, S., Kondo, K., Nabekawa, Y., Sagisaka, A. & Kobayashi, Y. Two-Color Phase Control in Tunneling Ionization and Harmonic Generation by a Strong Laser Field and Its Third Harmonic. *Phys. Rev. Lett.* **73**, 2692 (1994).
15. Kondo, K., Kobayashi, Y., Sagisaka, A., Nabekawa, Y. & Watanabe, S. Tunneling ionization and harmonic generation in two-color fields. *J. Opt. Soc. Am. B* **13**, 424–429 (1996).
16. Pi, L. W., Shi, T. Y. & Qiao, H. X. Enhancement of Bichromatic High-Order Harmonic Generation by a Strong Laser Field and Its Third Harmonic. *Chin. Phys. Lett.* **23**, 1490 (2006).
17. Ishikawa, K. Photoemission and Ionization of He^+ under Simultaneous Irradiation of Fundamental Laser and High-Order Harmonic Pulses. *Phys. Rev. Lett.* **91**, 043002 (2003).
18. Ivanov, I. A. & Kheifets, A. S. Tailoring the waveforms to extend the high-order harmonic generation cutoff. *Phys. Rev. A* **80**, 023809 (2009).
19. Chipperfield, L. E., Robinson, J. S., Tisch, J. W. G. & Marangos, J. P. Ideal waveform to generate the maximum possible electron recollision energy for any given oscillation period. *Phys. Rev. Lett.* **102**, 063003 (2009).
20. Schafer, K. J., Gaarde, M. B., Heinrich, A., Biegert, J. & Keller, U. Strong Field Quantum Path Control Using Attosecond Pulse Trains. *Phys. Rev. Lett.* **92**, 23003 (2004).
21. Gaarde, M. B., Schafer, K. J., Heinrich, A., Biegert, J. & Keller, U. Large enhancement of macroscopic yield in attosecond pulse train-assisted harmonic generation. *Phys. Rev. A* **72**, 013411 (2005).
22. Heinrich, A. *et al.* Enhanced VUV-assisted high harmonic generation. *J. Phys. B* **39**, S275 (2006).
23. Takahashi, E. J., Kanai, T., Ishikawa, K. L., Nabekawa, Y. & Midorikawa, K. Dramatic Enhancement of High-Order Harmonic Generation. *Phys. Rev. Lett.* **99**, 053904 (2007).
24. Lewenstein, M., Salières, P. & L'Huillier, A. Phase of the atomic polarization in high-order harmonic generation. *Phys. Rev. A* **52**, 4747 (1995).

25. Dahlström, J. M., L'Huillier, A. & Mauritsson, J. Quantum mechanical approach to probing the birth of attosecond pulses using a two-colour field. *J. Phys. B* **44**, 095602 (2011).
26. Erny, C. *et al.* Metrology of high-order harmonics for free-electron laser seeding. *New J. Phys.* **13**, 073035 (2011).
27. Heyl, C. M., Güdde, J., L'Huillier, A. & Höfer, U. High-order harmonic generation with μJ laser pulses at high repetition rates. *J. Phys. B* **45**, 074020 (2012).
28. Arnold, C. L. *et al.* Pulse compression with planar hollow waveguides: a pathway towards relativistic intensity with table-top lasers. *N. J. Phys.* **12**, 073015 (2010).
29. Takahashi, E., Nabekawa, Y. & Midorikawa, K. Generation of 10-μJ coherent extreme-ultraviolet light by use of high-order harmonics. *Opt. Lett.* **27**, 1920 (2002).
30. Salières, P., L'Huillier, A. & Lewenstein, M. Coherence control of high-order harmonics. *Phys. Rev. Lett.* **74**, 3776 (1995).

Acknowledgements

We thank Erik Mansten, Jörg Schwenke, and Rafal Rakowski for their early contribution to the project, and Byunghoon Kim for his contribution to the $\omega/3\omega$ measurements. This research was supported by the Marie Curie program ATTOFEL (ITN), the European Research Council (ALMA), the Joint Research Programme ALADIN of Laserlab-Europe II, the Swedish Research Council, the Swedish Foundation for Strategic Research, the Knut and Alice Wallenberg Foundation.

Author contributions

F.B., C.M.H. and P.R. contributed equally to this work. F.B., C.M.H., P.R. and L.R. performed the experiments. D.K. and C.L.A. performed the propagation calculations. C.M.H. and J.M.D. performed the SFA calculations. J.M, P.J., A.L. and all the other authors helped with the interpretation and the writing of the article.

Additional information

Competing financial interests: The authors declare no competing financial interests.

How to cite this article: Brizuela, F. *et al.* Efficient high-order harmonic generation boosted by below-threshold harmonics. *Sci. Rep.* **3**, 1410; DOI:10.1038/srep01410 (2013).